was concentrated and methanol-soluble portions (PM/SR-*-2) were obtained by washing the residue and concentration.

3.3. Screening for HCV NS3 Helicase Inhibitors

The fluorescence helicase assay based on FRET was performed as described in our previous study [23]. The dsRNA substrate was prepared by annealing the 5' Alexa Fluor 488 labeled fluorescence strand (5'-UAGUACCGCCACCCUCAGAACCUUUUUUUUUUUUUU-3') to the 3' BHQ1 labeled quencher strand (5'-GGUUCUGAGGGUGGCCCUACUA-3') at a 1:2 molar ratio. The dsRNA substrate has the 3'-overhang that is necessary for NS3 helicase to bind RNA prior to the duplex unwinding. The capture strand (5'-TAGTACCGCCACCCTCAGAACC-3'), which is complementary to the quencher strand, prevents the unwound duplexes from reannealing. None of the above three strands is self-complementary. The fluorescence and quencher strands were purchased from Japan Bio Services (Saitama, Japan). The capture strand was purchased from Tsukuba Oligo Service (Ibaraki, Japan). The reaction mixture contained 25 mM MOPS-NaOH (pH 6.5), 3 mM $MgCl_2$, 2 mM dithiothreitol, 4 U of RNasin (Promega, WI, USA), 50 nM dsRNA substrate, 100 nM capture strand, 5 mM ATP, an extract from a marine organism, and 240 nM NS3 in a total volume of 20 μL. Each extract from a marine organism diluted with DMSO was added to the reaction mixture at a final concentration in the range of 17.5–32.5 μg/mL. The full-length HCV NS3 protein with serine protease and ATPase/helicase was expressed and purified as described previously [23].

The reaction was started by adding HCV NS3 helicase and performed at 37 °C for 30 min using a LightCycler 1.5 (Roche Diagnostics, Basel, Switzerland). Fluorescence intensity was recorded every 5 s from 0 to 5 min, and then every 30 s from 5 to 30 min. Helicase activity was calculated as the initial reaction velocity relative to that of the control without a sample but with DMSO.

3.4. ATP Hydrolysis (ATPase) Assay

Following our previous report [26], unless otherwise stated, the standard assay reaction (10 μL) contained the following components: 25 mM MOPS-NaOH (pH 7.0), 1 mM DTT, 5 mM $MgCl_2$, 5 mM $CaCl_2$, 1 mM [γ-^{32}P] ATP, 300 nM NS3, and 0.1 μg/μL poly(U) with serial dilution of the tested compounds in DMSO. Samples were incubated at 37 °C for 10 min, and the reaction was terminated by adding 15 μL of stop solution (10 mM EDTA). A small portion (2 μL) of reaction mixture was spotted on a PEI-cellulose TLC plate (Merck Millipore, Darmstadt, Germany) and developed by ascending chromatography in 0.75 M LiCl/1 M formic acid solution for 25 min. The TLC plate was then air-dried, and applied to autoradiography measured by an Image Reader FLA-9000 and quantified by Multi Gauge V3.11 software (Fujifilm, Tokyo, Japan). For the bacterial alkaline phosphatase assay, the buffer provided with the kit (Takara Bio, Otsu, Japan) was used, and then subjected to the assay as described above.

3.5. Gel Mobility Shift Assay (GMSA)

GMSA was performed with slight modification as described previously [26]. In brief, [γ-^{32}P] ATP-labeled single-stranded RNA (0.4 nM) was incubated in a buffer containing 30 mM Tris-HCl pH 7.5,

100 mM NaCl, 2 mM $MgCl_2$, 1 mM DTT, 20 U of RNasin plus (Promega) in the presence of 300 nM NS3 protein with serial dilution of PBDE in DMSO at room temperature for 15 min in a final reaction volume of 20 μL. The protein-RNA complexes were loaded onto a 6% native-PAGE (acrylamide:bis = 19:1) and after electrophoresis in TBE buffer, the labeled RNA bands were visualized and quantified with an Image Reader FLA-9000 (Fujifilm) and Multi Gauge V3.11 software (Fujifilm), respectively.

3.6. HCV Replication Assay

The cell lines harboring the subgenomic replicon RNAs of genotype 1b strain N [27] were seeded at 2×10^4 cells per well in a 48-well plate 24 h before treatment. The cells were treated with PBDE at various concentrations for 72 h and lysed in cell culture lysis reagent (Promega). A luciferase assay system (Promega) was used to determine the luciferase activity, and the luminescence was measured using Luminescencer-JNR AB-2100 (ATTO, Tokyo, Japan), corresponding to the expression level of the HCV replicon.

3.7. Toxicity Assay

MTS assay was carried out to determine cytotoxicity using a CellTiter 96 aqueous one-solution cell proliferation assay kit (Promega) according to the manufacturer's instructions.

4. Conclusions

In conclusion, the present study showed that PBDE (**1**) isolated from a marine sponge inhibited NS3 helicase through suppression of the ATPase and RNA binding activities. Moreover, PBDE (**1**) did not inhibit bacterial alkaline phosphatase, suggesting that PBDE (**1**) is specific for NS3 inhibition. Structure-activity relationships demonstrated that the biphenyl ring, bromine, and phenolic hydroxyl group on the benzene backbone might be crucial groups essential for the inhibitory potency.

Acknowledgments

This work was supported by MEXT KAKEN 22603007.

Author Contributions

Conceived and designed the experiments: M.T., N.A., H.T., N.N., S.T., Y.S. Performed the experiments: K.A.S., A.F., A.Y. Analyzed the data: K.A.S., M.T., N.A., K.M., M.N. Wrote the paper: K.A.S., M.T., N.A. Collected and identified the marine sponge: J.T., S.R.R.

Conflicts of Interest

The authors declare no conflict of interest.

References

1. Choo, Q.L.; Kuo, G.; Weiner, A.J.; Overby, L.R.; Bradley, D.W.; Houghton, M. Isolation of a cDNA clone derived from a blood-borne non-A, non-B viral hepatitis genome. *Science* **1989**, *244*, 359–362.
2. Gravitz, L. Introduction: A smouldering public-health crisis. *Nature* **2011**, *474,* S2–S4.
3. Poordad, F.; McCone, J., Jr.; Bacon, B.R.; Bruno, S.; Manns, M.P.; Sulkowski, M.S.; Jacobson, I.M.; Reddy, K.R.; Goodman, Z.D.; Boparai, N.; *et al.* Boceprevir for untreated chronic HCV genotype 1 infection. *N. Engl. J. Med.* **2011**, *364*, 1195–1206.
4. Bacon, B.R.; Gordon, S.C.; Lawitz, E.; Marcellin, P.; Vierling, J.M.; Zeuzem, S.; Poordad, F.; Goodman, Z.D.; Sings, H.L.; Boparai, N.; *et al.* Boceprevir for previously treated chronic HCV genotype 1 infection. *N. Engl. J. Med.* **2011**, *364*, 1207–1217.
5. Jacobson, I.M.; McHutchison, J.G.; Dusheiko, G.; di bisceglie, A.M.; Reddy, K.R.; Bzowej, N.H.; Marcellin, P.; Muir, A.J.; Ferenci, P.; Flisiak, R.; *et al.* Telaprevir for previously untreated chronic hepatitis C virus infection. *N. Engl. J. Med.* **2011**, *364*, 2405–2416.
6. Zeuzem, S.; Andreone, P.; Pol, S.; Lawitz, E.; Diago, M.; Roberts, S.; Focaccia, R.; Younossi, Z.; Foster, G.R.; Horban, A.; *et al.* Telaprevir for retreatment of HCV infection. *N. Engl. J. Med.* **2011**, *364*, 2417–2428.
7. Takamizawa, A.; Mori, C.; Fuke, I.; Manabe, S.; Murakami, S.; Fujita, J.; Onishi, E.; Anodoh, T.; Yoshida, I.; Oakayama, H. Structure and organization of the hepatitis C virus genome isolated from human carriers. *J. Virol.* **1991**, *65*, 1105–1113.
8. Kai, L. Development of novel antiviral therapies for hepatitis C virus. *Virol. Sin.* **2010**, *25*, 246–266.
9. Moradpour, D.; Penin F.; Rice, C.M. Replication of hepatitis C virus. *Nat. Rev. Microbiol.* **2007**, *5*, 453–463.
10. Rice, C.M. New insights into HCV replication: Potential antiviral targets. *Top. Antivir. Med.* **2011**, *19*, 117–120.
11. De Francesco, R.; Steinkühler, C. Structure and function of the hepatitis C virus NS3-NS4A serine proteinase. *Curr. Top. Microbiol. Immunol.* **2000**, *242*, 149–169.
12. Raney, K.D.; Sharma, S.D.; Moustafa, I.M.; Cameron, C.E. Hepatitis C virus non-structural protein 3 (HCV NS3): A multifunctional antiviral target. *J. Biol. Chem.* **2010**, *285*, 22725–22731.
13. Ghany, M.G.; Nelson, D.R.; Strader, D.B.; Thomas, D.L.; Seeff, L.B. An update on treatment of genotype 1 chronic hepatitis C virus infection: 2011 practice guideline by the American Association for the Study of Liver Diseases. *Hepatology* **2011**, *54*, 1433–1444.
14. Hanif, N.; Tanaka, J.; Setiawan, A.; Trianto, A.; de Voogd, N.J.; Murni, A.; Tanaka, C.; Higa, T. Polybrominated diphenyl ethers from the Indonesian sponge *Lamellodysidea. herbacea. J. Nat. Prod.* **2007**, *70*, 432–435.
15. Sharma, G.M.; Vig, B. Studies on the antimicrobial substances of sponges. Structures of two antibacterial substances isolated from the marine sponge *Dysidea. Herbacea. Tetrahedron Lett.* **1972**, *17*, 1715–1718.
16. Salva, J.; Faulkner, D.J. A new brominated diphenyl ether from a Philippine *Dysidea.* species. *J. Nat. Prod.* **1990**, *53*, 757–760.

17. Handayani, D.; Edrada, R.A.; Proksch, P.; Wray, V.; Witte, L.; van Soest, R.W.; Kunzmann, A.; Soedarsono. Four new bioactive polybrominated diphenyl ethers of the sponge *Dysidea. herbacea* from West Sumatra, Indonesia. *J. Nat. Prod.* **1997**, *60*, 1313–1316.
18. Sionov, E.; Roth, D.; Sandovsky-Losica, H.; Kashman, Y.; Rudi, A.; Chill, L.; Berdicevsky, I.; Segal, E. Antifungal effect and possible mode of activity of a compound from the marine sponge *Dysidea. herbacea. J. Infect.* **2005**, *50*, 453–460.
19. Hattori, T.; Konno, A.; Adachi, K.; Shizuri, Y. Four new bioactive bromophenols from the palauan Sponge *Phyllospongia. dendyi. Fish. Sci.* **2001**, *67*, 899–903.
20. Fu, X.; Schmitz, F.J.; Govindan, M.; Abbas, S.A.; Hanson, K.M.; Horton, P.A.; Crews, P.; Laney, M.; Schatzman, R.C. Enzyme inhibitors: New and known polybrominated phenols and diphenyl ethers from four Indo-pacific *Dysidea.* sponges. *J. Nat. Prod.* **1995**, *58*, 1384–1391.
21. Liu, H.; Namikoshi, M.; Meguro, S.; Nagai, H.; Kobayashi, H.; Yao, X. Isolation and characterization of polybrominated diphenyl ethers as inhibitors of microtubule assembly from the marine sponge *Phyllospongia. dendyi* collected at Palau. *J. Nat. Prod.* **2004**, *67*, 472–474.
22. Xu, Y.; Johnson, R.K.; Hecht, S.M. Polybrominated diphenyl ethers from a sponge of the *Dysidea.* genus that inhibit Tie2 kinase. *Bioorg. Med. Chem.* **2005**, *13*, 657–659.
23. Tani, H.; Fujita, O.; Furuta, A.; Matsuda, Y.; Miyata, R.; Akimitsu, N.; Tanaka, J.; Tsuneda, S.; Sekiguchi, Y.; Noda, N. Real-time monitoring of RNA helicase activity using fluorescence resonance energy transfer *in vitro*. *Biochem. Biophys. Res. Commun.* **2010**, *393*, 131–136.
24. Suzich, J.A.; Tamura, J.K.; Palmer-Hill, F.; Warrener, P.; Grakoui, A.; Rice, CM.; Feinstone, S.M.; Collett, M.S. Hepatitis C virus NS3 protein polynucleotide-stimulated nucleoside triphosphatase and comparison with the related pestivirus and flavivirus enzymes. *J. Virol.* **1993**, *67*, 6152–6158.
25. Capon, R.; Ghisalberti, E.L.; Jefferies, P.R.; Skelton, B.W.; White, A.H. Structural studies of halogenated diphenyl ethers from a marine sponge. *J. Chem. Soc. Perkin Trans. 1.* **1981**, 2464–2467.
26. Salam, K.A.; Furuta, A.; Noda, N.; Tsuneda, S.; Sekiguchi, Y.; Yamashita, A.; Moriishi, K.; Nakakoshi, M.; Tsubuki, M.; Tani, H.; *et al.* Inhibition of hepatitis C virus NS3 helicase by manoalide. *J. Nat. Prod.* **2012**, *75*, 650–654.
27. Yokota, T.; Sakamoto, N.; Enomoto, N.; Tanabe, Y.; Miyagishi, M.; Maekawa, S.; Yi, L.; Kurosaki, M.; Taira, K.; Watanabe, M.; *et al.* Inhibition of intracellular hepatitis C virus replication by synthetic and vector-derived small interfering RNAs. *EMBO Rep.* **2003**, *4*, 602–608.

Sample Availability: Samples of the compounds are not available from the authors.

EFdA, a Reverse Transcriptase Inhibitor, Potently Blocks HIV-1 *Ex Vivo* Infection of Langerhans Cells within Epithelium

Journal of Investigative Dermatology advance online publication, 2 January 2014; doi:10.1038/jid.2013.467

TO THE EDITOR

Despite increasing access to antiretroviral drugs, sexual transmission of HIV-1 remains a significant public health threat. A recent clinical trial, CAPRISA 004, of a vaginally administered microbicide using a nucleoside reverse transcriptase inhibitor (NRTI), tenofovir (TDF), has demonstrated that 1% TDF gel reduced HIV-1 acquisition by an estimated 39% overall (Abdool Karim *et al.*, 2010), indicating a potential utility of NRTI-based microbicides. In the VOICE study, however, a once-daily dosing regimen with TDF gel failed to demonstrate protective effects in at-risk women. These studies demonstrate the need to develop additional more potent microbicide candidates to potentially increase the activity to protect women from HIV-1 transmission.

We previously reported that a series of 4′-substituted NRTIs have excellent antiviral properties (Ohrui, 2006), and through optimization of such 4′-substituted NRTIs, 4′-ethynyl-2-fluoro-2′-deoxyadenosine (EFdA) was found to exert extremely potent activity against a wide spectrum of HIV-1 strains including highly multidrug-resistant clinical HIV-1 isolates, with favorable *in vitro* cell toxicities (Nakata *et al.*, 2007; Ohrui *et al.*, 2007). EFdA inhibited HIV-1 replication in activated peripheral blood mononuclear cells with an EC_{50} of 0.05 nM, a potency several orders of magnitude greater than any of the current clinically available NRTIs (Michailidis *et al.*, 2009). As the prevalence of new infections with drug-resistant HIV-1 variants could increase in the coming years (Nichols *et al.*, 2011), EFdA may be useful as a topical microbicide.

Langerhans cells (LCs) are dendritic cells located, among other sites, within genital skin and mucosal epithelium (Lederman *et al.*, 2006). In female rhesus macaques exposed intravaginally to simian immunodeficiency virus, up to 90% of initially infected target cells were LCs (Hu *et al.*, 2000). *Ex vivo* experiments with human foreskin explants show that epidermal LCs in inner foreskin are primary target cells for HIV-1 infection, providing a plausible explanation for why circumcision greatly reduces the probability of acquiring HIV-1 (Ganor *et al.*, 2010; Zhou *et al.*, 2011). LCs also express CD4 and CCR5, but not CXCR4, and demonstrate the distinctive characteristics of emigrating from tissue to draining lymph nodes in order to interact with T cells following contact with pathogens (Lederman *et al.*, 2006). Indeed, epidermal LCs are readily infected *ex vivo* with R5-HIV-1, but not with X4-HIV-1, and initiate and promote high levels of infection upon interactions with cocultured $CD4^+$ T cells (Kawamura *et al.*, 2000; Ogawa *et al.*, 2009, 2013), consistent with previous epidemiologic observations that the majority of HIV-1 strains isolated from newly infected patients are R5-HIV-1 strains (Zhu *et al.*, 1993). Thus, LCs likely have an important role in disseminating HIV-1 soon after exposure to the virus.

To understand how HIV-1 traverses skin and genital mucosa, an *ex vivo* model was developed in which resident LCs within epithelial tissue explants obtained from suction blisters are exposed to HIV-1 and then allowed to emigrate from the tissue, thus mimicking conditions that occur following mucosal exposure to HIV (Kawamura *et al.*, 2000; Ogawa *et al.*, 2009, 2013). In this model, although relatively few productively infected LCs are identified, these cells induce high levels of HIV-1 infection when cocultured with resting autologous $CD4^+$ T cells (Kawamura *et al.*, 2000; Ogawa *et al.*, 2013). As expected, when epidermal tissue explants were pretreated with various concentrations of TDF, EFdA, and CCR5 inhibitor, maraviroc (MVC), prior to R5-tropic $HIV\text{-}1_{Ba\text{-}L}$ exposure, HIV-1 infection of resident LCs within epidermis as well as subsequent virus transmission from emigrated LCs to cocultured $CD4^+$ T cells was decreased in a dose-dependent manner (Figure 1a and c; for detailed methods, see Supplementary Material). The blocking was confirmed by repeated experiments using skin explants from three additional randomly selected individuals (Figure 1b and d). Strikingly, although the blocking efficiency of TDF or MVC even at 5,000 nM was partial, EFdA demonstrated complete blocking of R5-HIV-1 replication in LCs as well as subsequent virus transmission from emigrated LCs to $CD4^+$ T cells at doses of 100–5,000 nM (Figure 1a–d). Furthermore, EFdA blocked *ex vivo* virus infection of LCs as well as subsequent virus transmission when two strains of R5-HIV-1, $HIV\text{-}1_{JR\text{-}FL}$ and $HIV\text{-}1_{AD8}$, were utilized in experiments ($n=3$, Supplementary Figure S1 online).

Similar to the results in epidermal LCs, preincubation of monocyte-derived LCs (mLCs) with 100–5,000 nM of EFdA

Abbreviations: EFdA, 4′-ethynyl-2-fluoro-2′-deoxyadenosine; LC, Langerhans cell; mLC, monocyte-derived LC; MVC, maraviroc; NRTI, nucleoside reverse transcriptase inhibitor; TDF, tenofovir

Accepted article preview online 11 November 2013

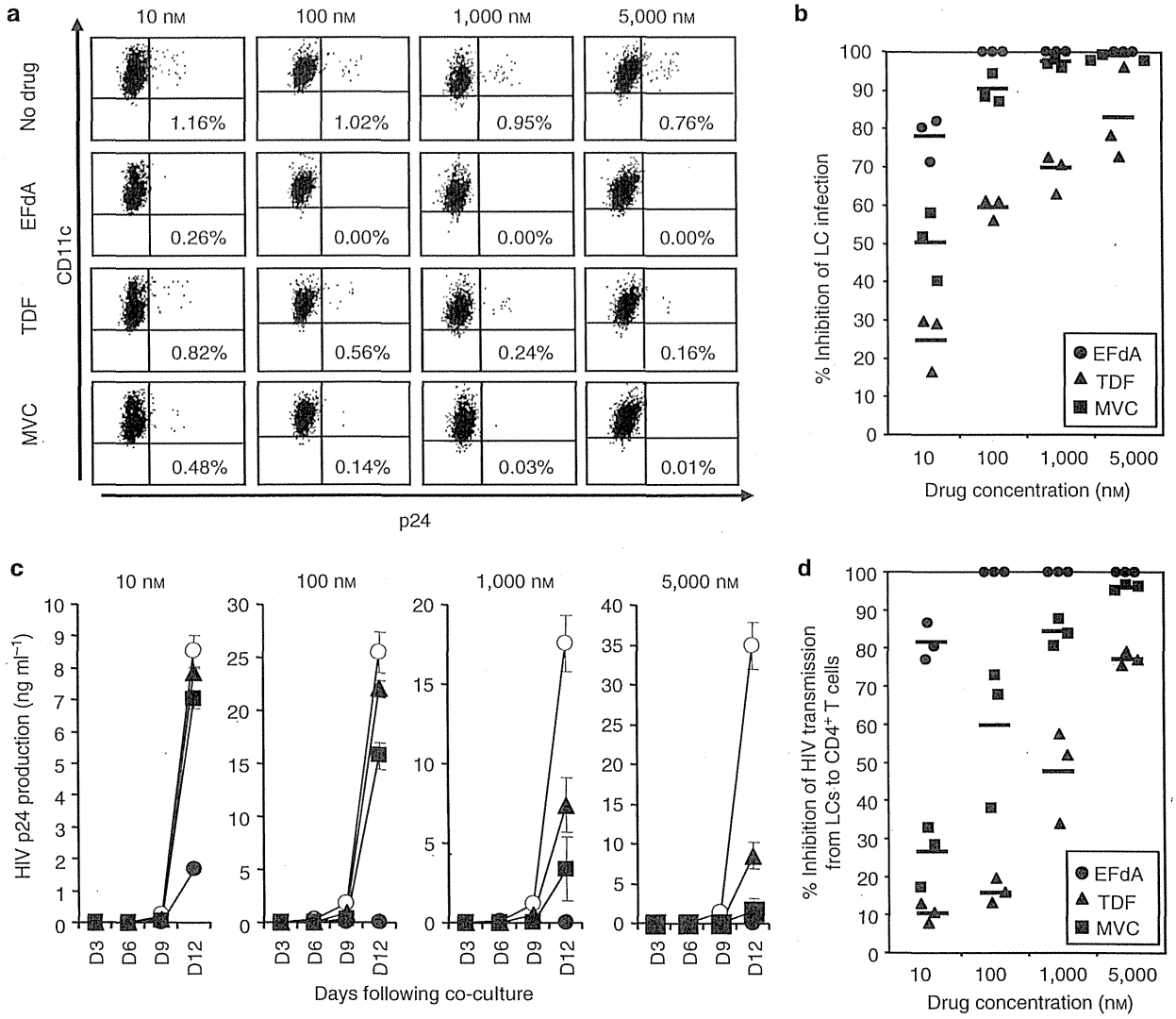

Figure 1. Preincubation of skin explants with EFdA blocks R5-HIV-1 infection in LCs and subsequent virus transmission to cocultured CD4$^+$ T cells. LCs within skin explants were preincubated with no drug (○) or the indicated concentrations of EFdA (●), TDF (▲), and MVC (■) for 30 minutes, exposed to HIV-1_{Ba-L} for 2 hours, and then floated on culture medium to allow migration of LCs from the explants. Emigrating cells from the epidermal sheets were collected 3 days following HIV-1 exposure. HIV-1-infected LCs were assessed by HIV-1 p24 intracellular staining in langerin$^+$ CD11c$^+$ LCs (**a**, **b**), or further cocultured with autologous CD4$^+$ T cells and culture supernatants were assessed for p24 content by ELISA on the indicated days (**c**, **d**). Summary of percent inhibition of LC infection (**b**) and virus transmission to CD4$^+$ T cells (**d**) of 12 experiments using skin explants from 12 individuals with the indicated each concentration of EFdA (●), TDF (▲), and MVC (■) are shown. Mean values obtained from different donors are shown as horizontal marks (**b**, **d**). EFdA, 4′-ethynyl-2-fluoro-2′-deoxyadenosine; LCs, Langerhans cells; MVC, maraviroc; TDF, tenofovir.

completely blocked HIV-1 replication in mLCs as well as subsequent virus transmission from mLCs to cocultured CD4$^+$ T cells, whereas both TDF and MVC at the same doses only partially inhibited the transmission (Figure 2a and b; for detailed methods, see Supplementary Material online). Intriguingly, even in 1–3 days following the removal of EFdA (1,000 nM), EFdA completely blocked HIV-1 infection of mLCs as well as subsequent virus transmission from mLCs to cocultured CD4$^+$ T cells, whereas TDF and MVC rapidly lost their anti-HIV-1 activity within days (Figure 2c–f). No cellular toxicity was noted for any of these drugs at the doses used in these experiments (Supplementary Figure S2 online). When similar experiments were conducted using peripheral blood mononuclear cell as target cells, virtually identical favorable persistency of EFdA in antiviral activity compared with that of TDF was observed (data not shown).

In the present work, we demonstrated that EFdA exerted extremely more potent anti-HIV-1 activity in LCs than did TDF and MVC, and the potent anti-HIV-1 activity of EFdA persisted for at least 3 days. Of note, the efficacy of TDF gel in CAPRISA 004 has been linked to its long intracellular half-life (Abdool Karim *et al.*, 2010; Rohan *et al.*, 2010). Our data strongly

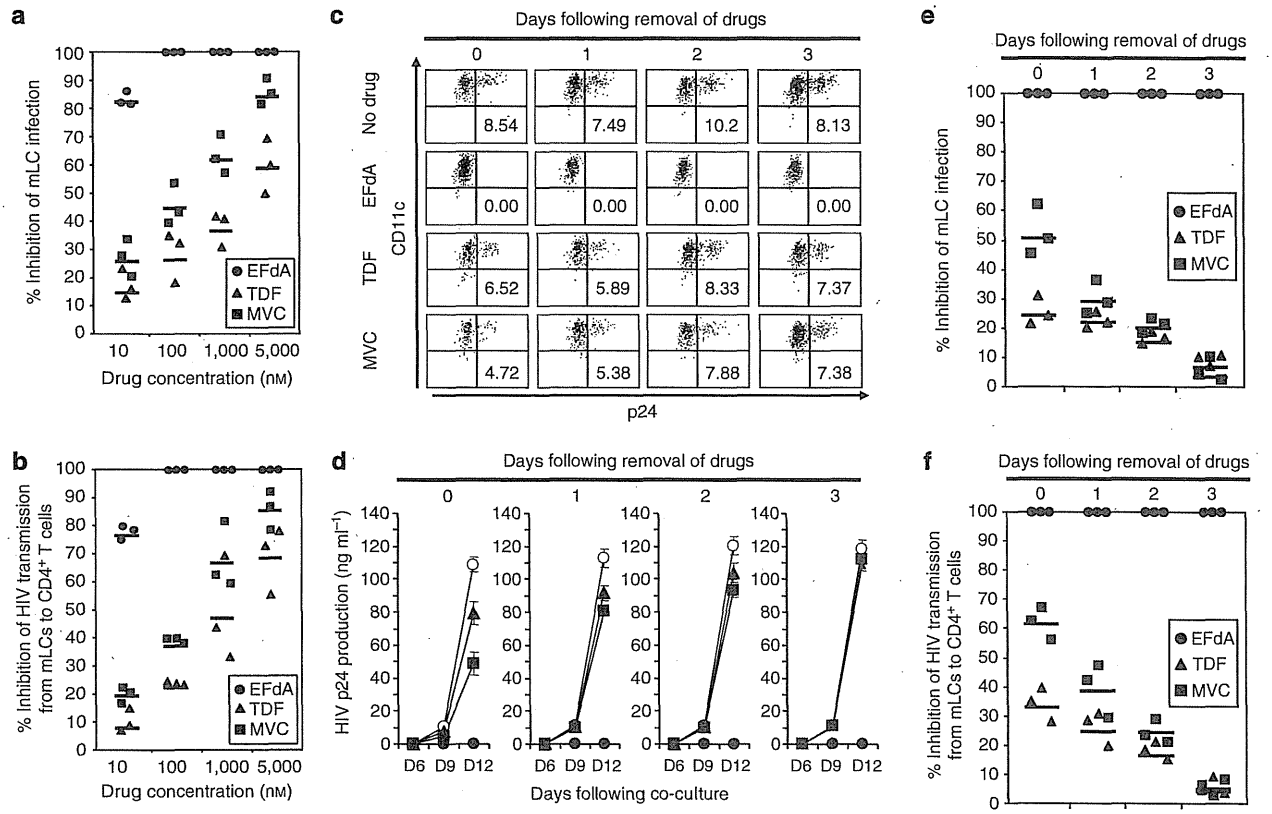

Figure 2. Preincubation of skin explants with EFdA blocks subsequent R5-HIV-1 infection in LC in a dose-dependent manner. mLCs were preincubated with no drug (○) or the indicated concentrations of EFdA (●), TDF (▲) and MVC (■) for 30 minutes, and then immediately exposed to HIV-1Ba-L for 2 hours (**a**, **b**), or thoroughly washed to remove the extracellular drug and further cultured for 1, 2, or 3 days prior to exposure to HIV-1Ba-L for 2 hours (**c**–**f**). After 7 days of HIV-1 exposure, HIV-1-infected mLCs were assessed by HIV-1 p24 intracellular staining in langerin$^+$ CD11c$^+$ mLCs (**a**, **c**, **e**), or further cocultured with autologous CD4$^+$ T cells and culture supernatants were assessed for p24 content by ELISA on the indicated days (**b**, **d**, **f**). Summary of percent inhibition of mLC infection (**a**, **e**) and virus transmission to CD4$^+$ T cells (**b**, **f**) of three independent experiments are shown. Mean values are shown as horizontal marks (**a**, **b**, **e**, **f**). EFdA, 4′-ethynyl-2-fluoro-2′-deoxyadenosine; LCs, Langerhans cells; mLCs, monocyte-derived LCs; MVC, maraviroc; TDF, tenofovir.

indicate that EFdA may serve as a promising microbicide to block sexual transmission of HIV-1 because of its potent anti-HIV-1 activity, low cytotoxicity, and superior persistence of antiviral activity against HIV-1 in LCs.

CONFLICT OF INTEREST

HM is among coinventors on a patent for EFdA; all rights, title, and interest to the patent have been assigned to Yamasa Corporation, Chiba, Japan. The other authors state no conflict of interest.

ACKNOWLEDGMENTS

Financial support was provided by the Ministry of Health Science of the Japanese Government (201029002), the Intramural Research Program of Center for Cancer Research, National Cancer Institute, National Institutes of Health, and a grant for global education and research center aiming at the control of AIDS (Global Center of Excellence supported by Monbu-Kagakusho).

Takamitsu Matsuzawa[1], Tatsuyoshi Kawamura[1], Youichi Ogawa[1], Kenji Maeda[2], Hirotomo Nakata[3], Kohji Moriishi[4], Yoshio Koyanagi[5], Hiroyuki Gatanaga[6], Shinji Shimada[1] and Hiroaki Mitsuya[2,3]

[1]Faculty of Medicine, Department of Dermatology, University of Yamanashi, Yamanashi, Japan; [2]Experimental Retrovirology Section, HIV and AIDS Malignancy Branch, National Cancer Institute, National Institutes of Health, Bethesda, Maryland, USA; [3]Department of Infectious Diseases and Hematology, Kumamoto University School of Medicine, Kumamoto, Japan; [4]Faculty of Medicine, Department of Microbiology, University of Yamanashi, Yamanashi, Japan; [5]Laboratory of Viral Pathogenesis, Institute for Virus Research, Kyoto University, Kyoto, Japan and [6]AIDS Clinical Center, National Center for Global Health and Medicine, Tokyo, Japan
E-mail: tkawa@yamanashi.ac.jp

SUPPLEMENTARY MATERIAL

Supplementary material is linked to the online version of the paper at http://www.nature.com/jid

REFERENCES

Abdool Karim Q, Abdool Karim SS, Frohlich JA *et al.* (2010) Effectiveness and safety of tenofovir gel, an antiretroviral microbicide, for the prevention of HIV infection in women. *Science* 329:1168–74

Ganor Y, Zhou Z, Tudor D *et al.* (2010) Within 1 h, HIV-1 uses viral synapses to enter efficiently the inner, but not outer, foreskin mucosa and engages Langerhans-T cell conjugates. *Mucosal Immunol* 3:506–22

Hu J, Gardner MB, Miller CJ (2000) Simian immunodeficiency virus rapidly penetrates the cervicovaginal mucosa after intravaginal inoculation and infects intraepithelial dendritic cells. *J Virol* 74:6087–95

Kawamura T, Cohen SS, Borris DL *et al.* (2000) Candidate microbicides block HIV-1 infection of human immature Langerhans cells within

epithelial tissue explants. *J Exp Med* 192: 1491–500

Lederman MM, Offord RE, Hartley O (2006) Microbicides and other topical strategies to prevent vaginal transmission of HIV. *Nat Rev Immunol* 6:371–82

Michailidis E, Marchand B, Kodama EN *et al.* (2009) Mechanism of inhibition of HIV-1 reverse transcriptase by 4′-Ethynyl-2-fluoro-2′-deoxyadenosine triphosphate, a translocation-defective reverse transcriptase inhibitor. *J Biol Chem* 284:35681–91

Nakata H, Amano M, Koh Y *et al.* (2007) Activity against human immunodeficiency virus type 1, intracellular metabolism, and effects on human DNA polymerases of 4′-ethynyl-2-fluoro-2′-deoxyadenosine. *Antimicrob Agents Chemother* 51:2701–8

Nichols BE, Boucher CA, van de Vijver DA (2011) HIV testing and antiretroviral treatment strategies for prevention of HIV infection: impact on antiretroviral drug resistance. *J Intern Med* 270:532–49

Ogawa Y, Kawamura T, Kimura T *et al.* (2009) Gram-positive bacteria enhance HIV-1 susceptibility in Langerhans cells, but not in dendritic cells, via Toll-like receptor activation. *Blood* 113:5157–66

Ogawa Y, Kawamura T, Matsuzawa T *et al.* (2013) Antimicrobial peptide LL-37 produced by HSV-2-infected keratinocytes enhances HIV infection of Langerhans cells. *Cell Host Microbe* 13:77–86

Ohrui H (2006) 2′-deoxy-4′-C-ethynyl-2-fluoro-adenosine, a nucleoside reverse transcriptase inhibitor, is highly potent against all human immunodeficiency viruses type 1 and has low toxicity. *Chem Rec* 6:133–43

Ohrui H, Kohgo S, Hayakawa H *et al.* (2007) 2′-Deoxy-4′-C-ethynyl-2-fluoroadenosine: a nucleoside reverse transcriptase inhibitor with highly potent activity against wide spectrum of HIV-1 strains, favorable toxic profiles, and stability in plasma. *Nucleosides, Nucleotides Nucleic Acids* 26: 1543–6

Rohan LC, Moncla BJ, Kunjara Na Ayudhya RP *et al.* (2010) *In vitro* and *ex vivo* testing of tenofovir shows it is effective as an HIV-1 microbicide. *PLoS One* 5:e9310

Zhou Z, Barry de Longchamps N, Schmitt A *et al.* (2011) HIV-1 efficient entry in inner foreskin is mediated by elevated CCL5/RANTES that recruits T cells and fuels conjugate formation with Langerhans cells. *PLoS Pathog* 7:e1002100

Zhu T, Mo H, Wang N *et al.* (1993) Genotypic and phenotypic characterization of HIV-1 patients with primary infection. *Science* 261: 1179–81

Mar. Drugs **2014**, *12*, 462-476; doi:10.3390/md12010462

OPEN ACCESS

marine drugs

ISSN 1660-3397

www.mdpi.com/journal/marinedrugs

Article

Identification and Biochemical Characterization of Halisulfate 3 and Suvanine as Novel Inhibitors of Hepatitis C Virus NS3 Helicase from a Marine Sponge

Atsushi Furuta [1,2], Kazi Abdus Salam [3], Idam Hermawan [4], Nobuyoshi Akimitsu [3], Junichi Tanaka [4], Hidenori Tani [5], Atsuya Yamashita [6], Kohji Moriishi [6], Masamichi Nakakoshi [7], Masayoshi Tsubuki [7], Poh Wee Peng [8], Youichi Suzuki [8], Naoki Yamamoto [8], Yuji Sekiguchi [2], Satoshi Tsuneda [1,*] and Naohiro Noda [1,2,*]

1 Department of Life Science and Medical Bioscience, Waseda University, 2-2 Wakamatsu-cho, Shinjuku-ku, Tokyo 162-8480, Japan; E-Mail: atsushi.5961@ruri.waseda.jp

2 Biomedical Research Institute, National Institute of Advanced Industrial Science and Technology (AIST), 1-1-1 Higashi, Tsukuba, Ibaraki 305-8566, Japan; E-Mail: y.sekiguchi@aist.go.jp

3 Radioisotope Center, The University of Tokyo, 2-11-16 Yayoi, Bunkyo-ku, Tokyo 113-0032, Japan; E-Mails: salam_bio26@yahoo.com (K.A.S.); akimitsu@ric.u-tokyo.ac.jp (N.A.)

4 Department of Chemistry, Biology and Marine Science, University of the Ryukyus, Nishihara, Okinawa 903-0213, Japan; E-Mails: damz_98@yahoo.com (I.H.); jtanaka@sci.u-ryukyu.ac.jp (J.T.)

5 Research Institute for Environmental Management Technology, National Institute of Advanced Industrial Science and Technology (AIST), 16-1 Onogawa, Tsukuba, Ibaraki 305-8569, Japan; E-Mail: h.tani@aist.go.jp

6 Department of Microbiology, Division of Medicine, Graduate School of Medicine and Engineering, University of Yamanashi, 1110 Shimokato, Chuo-shi, Yamanashi 409-3898, Japan; E-Mails: atsuyay@yamanashi.ac.jp (A.Y.); kmoriishi@yamanashi.ac.jp (K.M.)

7 Institute of Medical Chemistry, Hoshi University, 2-4-41 Ebara, Shinagawa-ku, Tokyo 142-8501, Japan; E-Mails: mnakako@hoshi.ac.jp (M.N.); tsubuki@hoshi.ac.jp (M.T.)

8 Department of Microbiology, Yong Loo Lin School of Medicine, National University of Singapore, Center for Translational Medicine, 14 Medical Drive, #15-02, Level 15, Singapore 117599, Singapore; E-Mails: micpwp@nus.edu.sg (P.W.P.); micys@nus.edu.sg (Y.S.); naoki_yamamoto@nuhs.edu.sg (N.Y.)

* Authors to whom correspondence should be addressed; E-Mails: stsuneda@waseda.jp (S.T.); noda-naohiro@aist.go.jp (N.N.); Tel.: +81-3-5369-7325 (S.T.); Fax: +81-3-3341-2684 (S.T.); Tel.: +81-29-861-6026 (N.N.); Fax: +81-29-861-6400 (N.N.).

Received: 20 December 2013; in revised form: 2 January 2014 / Accepted: 10 January 2014 / Published: 21 January 2014

Abstract: Hepatitis C virus (HCV) is an important etiological agent that is responsible for the development of chronic hepatitis, liver cirrhosis, and hepatocellular carcinoma. HCV nonstructural protein 3 (NS3) helicase is a possible target for novel drug development due to its essential role in viral replication. In this study, we identified halisulfate 3 (hal3) and suvanine as novel NS3 helicase inhibitors, with IC_{50} values of 4 and 3 μM, respectively, from a marine sponge by screening extracts of marine organisms. Both hal3 and suvanine inhibited the ATPase, RNA binding, and serine protease activities of NS3 helicase with IC_{50} values of 8, 8, and 14 μM, and 7, 3, and 34 μM, respectively. However, the dengue virus (DENV) NS3 helicase, which shares a catalytic core (consisting mainly of ATPase and RNA binding sites) with HCV NS3 helicase, was not inhibited by hal3 and suvanine, even at concentrations of 100 μM. Therefore, we conclude that hal3 and suvanine specifically inhibit HCV NS3 helicase via an interaction with an allosteric site in NS3 rather than binding to the catalytic core. This led to the inhibition of all NS3 activities, presumably by inducing conformational changes.

Keywords: marine organism; halisulfate 3; suvanine; hepatitis C virus; NS3 helicase; dengue virus

1. Introduction

An estimated 150 million people worldwide are chronically infected with the hepatitis C virus (HCV), a major etiological agent responsible for the development of chronic hepatitis, liver cirrhosis, and hepatocellular carcinoma (World Health Organization, 2013). The current standard therapy is based mainly on a triple combination of pegylated interferon-alfa, ribavirin, and a recently approved NS3 serine protease inhibitor (such as telaprevir), which increases the viral clearance rate to >70% [1,2]. However, because of severe side effects, the emergence of drug-resistant HCV mutations, and drug-drug interactions [3,4], the development of novel direct-acting antivirals that target the viral or host proteins involved in HCV replication are needed urgently. HCV nonstructural protein 3 (NS3) helicase has been considered as a novel antiviral target owing to its essential role in viral replication [5,6].

HCV is a member of the *Flaviviridae* family of positive-stranded RNA viruses. The viral genome contains a single open reading frame encoding a polyprotein that is processed by virus-encoded and host cellular proteases into structural and nonstructural proteins. The structural proteins (core protein [C], and the envelope glycoproteins E1 and E2) build up the virus particle, whereas the nonstructural proteins p7 and NS2 support particle assembly without being incorporated into the viral particles [7,8]. The remaining nonstructural proteins (NS3, NS4A, NS4B, NS5A, and NS5B) form a complex with viral RNA to support viral replication [9]. NS3 is a multifunctional enzyme with serine protease and NTPase/helicase domains at the *N*- and *C*-termini, respectively [10]. The NS3 helicase can unwind double-stranded RNA (dsRNA), double-stranded DNA, and RNA/DNA heteroduplexes in a 3′–5′ direction by using a nucleoside triphosphate as the energy source [11–14]. Although the exact role of NS3 helicase in the viral life cycle remains unclear, a fully functional NS3 helicase is required for replication of the HCV replicon [5] and for HCV replication in chimpanzees [15], suggesting that NS3

helicase inhibitors could be potential therapeutic agents. However, no HCV NS3 helicase inhibitors have yet been entered into clinical trials, at least in part due to similarities between NS3 and cellular RNA helicases [8].

HCV NS3 helicase is part of the family of viral DExH proteins; the NS3/NPH-II family that encompasses helicases from positive-stranded RNA viruses [16–18]. These closely related helicases share a catalytic core that consists mainly of NTPase and nucleic acid binding sites, as well as many other structural and functional features. Indeed, dengue virus (DENV) NS3 helicase, another viral DExH protein, and HCV NS3 helicase share highly conserved amino acid sequences, and consequently have similar conformational structures [19]. Thus, if a compound inhibits HCV NS3 helicase, it may also inhibit DENV NS3 helicase [20–22]. Assessing the inhibitory specificity can provide useful information to understand whether inhibitors target the NTPase, nucleic acid binding, or other allosteric sites of NS3 helicase.

HCV NS3 helicase inhibitors function by inhibiting NTP binding, nucleic acid binding, NTP hydrolysis or NDP release, the coupling of NTP hydrolysis to the translocation and unwinding of nucleic acids, or unwinding by sterically blocking helicase translocation [6]. In addition, owing to an interdependent linkage between NS3 helicase and serine protease activities [23–25], the inhibition of NS3 serine protease may also lead to the inhibition of NS3 helicase. Compounds that intercalate into the strands of double-stranded nucleic acids could also inhibit NS3 helicase [26].

Naturally occurring products are an important source of structurally diverse and biologically active secondary metabolites. The diversity of organisms in the marine environment has provided new drugs in almost all therapeutic areas [27–29]. To date, seven therapeutic agents derived from the marine environment are used as anticancer, antiviral, pain control, and hypertriglyceridemia agents [27]. The chemical structure has been isolated for two of these compounds, whereas the remaining five are synthetic agents based on marine products. An additional 13 agents are in phase 1, 2, or 3 clinical trials. Therefore, natural marine products include a number of highly significant lead compounds that are driving new drug development.

In this study, we screened extracts from marine organisms for NS3 helicase inhibitors using a fluorescence helicase assay based on photoinduced electron transfer (PET), as described in our previous study [30]. During purification, halisulfate 3 (hal3) and suvanine, which were isolated from marine sponge extracts, were identified as novel NS3 helicase inhibitors with IC_{50} values in the low micromolar range. The inhibitory effects of hal3 and suvanine against the other helicase-related activities of NS3 (ATPase, RNA binding, and serine protease activities) were also assessed. Finally, the inhibitory activities of hal3 and suvanine against DENV NS3 helicase were determined to characterize the binding sites of hal3 and suvanine.

2. Results and Discussion

To obtain novel NS3 helicase inhibitors, extracts from marine organisms were screened using a fluorescence helicase assay based on PET. Forty-three extracts prepared from marine organisms were screened, and 11 were identified that inhibited the helicase activity >50% (samples 4, 10, 13, 14, 17, 19, 21, 22, 25, 26, and 37) (Table 1), suggesting that these extracts contained NS3 helicase inhibitors. Of these extracts, sample 10 exhibited the strongest inhibition of NS3 helicase, and abolished its

activity completely. Therefore, this extract was purified to isolate and concentrate the inhibitory components. After several purification steps, the inhibitory components were identified as hal3 and suvanine (Figure 1) by comparing their NMR spectra with those reported previously [31,32] for each compound (Supplementary Figures S1–S4). Hal3 and suvanine inhibited NS3 helicase activity in a dose-dependent manner, with IC_{50} values of 4 and 3 μM, respectively (Figure 2A,B).

Table 1. Inhibitory effects of extracts from marine organisms on hepatitis C virus (HCV) nonstructural protein 3(NS3) helicase activity.

No.	NS3 Helicase Activity (% of Control) *	Marine Organism	Species
1	92	Sponge	*Unidentified*
2	74	Soft coral	*Briareum*
3	57	Tunicate	*Unidentified*
4	36	Sponge	*Liosina*
5	54	Sponge	*Unidentified*
6	71	Sponge	*Xestospongia*
7	77	Sponge	*Epipolasis*
8	110	Sponge	*Unidentified*
9	86	Sponge	*Strongylophora*
10	**0**	**Sponge**	***Unidentified***
11	83	Sponge	*Stylotella aurantium*
12	78	Sponge	*Epipolasis*
13	25	Sponge	*Unidentified*
14	43	Sponge	*Hippospongia*
15	75	Sponge	*Unidentified*
16	85	Sponge	*Unidentified*
17	49	Sponge	*Xestospongia testudinaria*
18	69	Sponge	*Unidentified*
19	40	Sponge	*Theonella*
20	64	Sponge	*Unidentified*
21	44	Sponge	*Unidentified*
22	46	Sponge	*Petrosia*
23	72	Tunicate	*Unidentified*
24	61	Sponge	*Unidentified*
25	50	Tunicate	*Didemnum molle*
26	33	Sponge	*Unidentified*
27	67	Sponge	*Unidentified*
28	87	Soft coral	*Unidentified*
29	62	Sponge	*Unidentified*
30	60	Sponge	*Unidentified*
31	85	Sponge	*Cinachyra*
32	70	Sponge	*Liosina*
33	68	Sponge	*Unidentified*
34	58	Sponge	*Unidentified*
35	72	Sponge	*Stylotella*
36	57	Sponge	*Unidentified*
37	39	Sponge	*Unidentified*

Table 1. *Cont.*

38	72	Tunicate	*Didemnum*
39	62	Sponge	*Unidentified*
40	71	Jellyfish	*Unidentified*
41	74	Sponge	*Unidentified*
42	52	Tunicate	*Unidentified*
43	67	Annelid	*Unidentified*

* NS3 helicase activity in the presence of extract is expressed as a percentage of control in the absence of extract (100%); The sample with the strongest inhibition against NS3 helicase is in bold, underlined font; samples with relatively strong inhibition against NS3 helicase (<50%) are underlined.

Figure 1. Structures of halisulfate 3 (hal3) and suvanine.

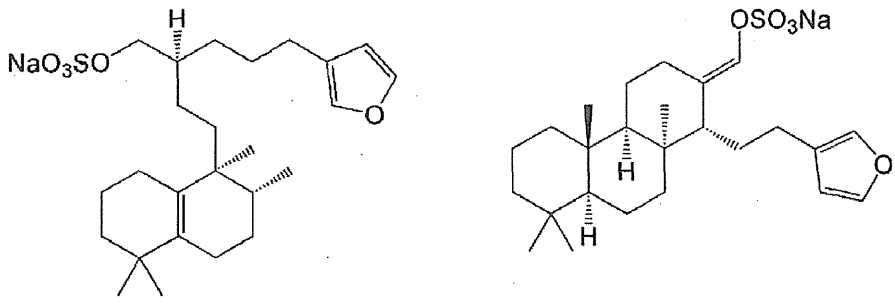

Halisulfate 3 Suvanine

The inhibitory effects of hal3 and suvanine were confirmed using a gel-based helicase assay. The helicase activity was calculated as the ratio of the signal intensity derived from single-stranded (ssRNA) in the sample containing the inhibitor to the control sample (lacking the inhibitor but containing DMSO vehicle). Similar to the results of the fluorescence helicase assay, hal3 and suvanine inhibited helicase-catalyzed RNA unwinding in a dose-dependent manner (Figure 2C,D). Therefore, these data clearly indicate that hal3 and suvanine exert inhibitory effects. Hal3 and suvanine were identified in 1988 [33] and 1985 [34], respectively. They have similar distinguishing structural features of a sulfated side chain and a furan moiety at the terminus of the molecule (Figure 1). Although some bioactivities for hal3 and suvanine have been reported, this report is the first that identifies these compounds as helicase inhibitors. In addition, bioactive effects of hal3 alone have not been reported. A mixture of halisulfates 2–5 (hal3 and its analogues) showed antimicrobial activity against *S. aureus*, *C. albicans*, and *B. subtilis*. Moreover, a mixture of halisulfates 2–4 inhibited PMA-induced inflammation in a mouse ear edema assay and inhibited phospholipase A_2 [31]. Suvanine is a serine protease inhibitor [35] and an antagonist of the mammalian bile acid sensor farnesoid-X-receptor [36]. In addition, suvanine interferes with heat shock protein 60, a chaperone involved in the inflammatory response, giving evidence for its anti-inflammatory properties [37].

Figure 2. Inhibition of NS3 helicase-catalyzed RNA unwinding activity by hal3 and suvanine. (**A**,**B**) Inhibition curves of hal3 and suvanine generated using a fluorescence helicase assay. The NS3 helicase activities of samples containing inhibitor were calculated relative to control samples containing DMSO vehicle rather than inhibitor. The data are presented as mean ± standard deviation of three replicates; (**C**,**D**) Gel images representing the inhibitory effects of hal3 and suvanine in a gel-based helicase assay. Fluorescence-labeled ssRNA and dsRNA were applied to lanes *1* and *2*, respectively. The dsRNA was incubated with NS3 in the presence of increasing concentrations of inhibitor (lanes *3*–*7*, 0–100 μM). Lane *8* shows the control reaction in the absence of NS3.

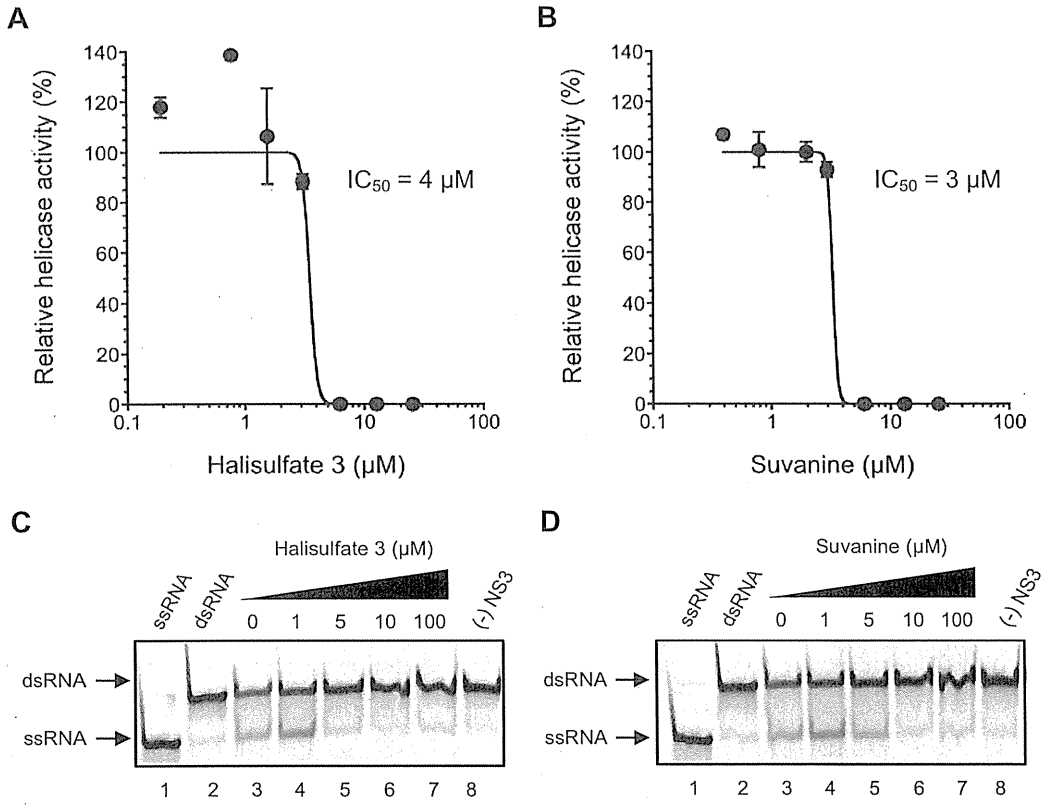

As the unwinding ability of NS3 helicase is dependent on ATP hydrolysis, the amount of inorganic phosphate (Pi) released from radioisotope-labeled ATP was measured to determine the effects of hal3 and suvanine on the ATPase activity of NS3 (Figure 3). The released Pi was separated by thin-layer chromatography and visualized using autoradiography. The density of the upper spots corresponding to Pi, which represents ATPase activity, decreased dose-dependently for both hal3 and suvanine. The ATPase activity was calculated as the ratio of the signal intensity derived from the released Pi in the sample containing inhibitor to that in the control sample (lacking the inhibitor but containing DMSO vehicle). The IC_{50} values of hal3 and suvanine were calculated to be 8 and 7 μM, respectively. As this concentration range is similar to that in which RNA unwinding was inhibited (Figure 2), it is likely that hal3 and suvanine inhibit NS3 helicase via the inhibition of ATPase activity.

Figure 3. Effects of hal3 and suvanine on NS3 ATPase activity demonstrated by autoradiography of an ATPase assay using [γ-^{32}P] ATP. Lane *1* contains the control reaction without NS3. Lanes *2–8* (**A**) and *2–9* (**B**) show the ATP hydrolysis reaction with poly(U) RNA at increasing concentrations (0–100 μM) of hal3 and suvanine, respectively.

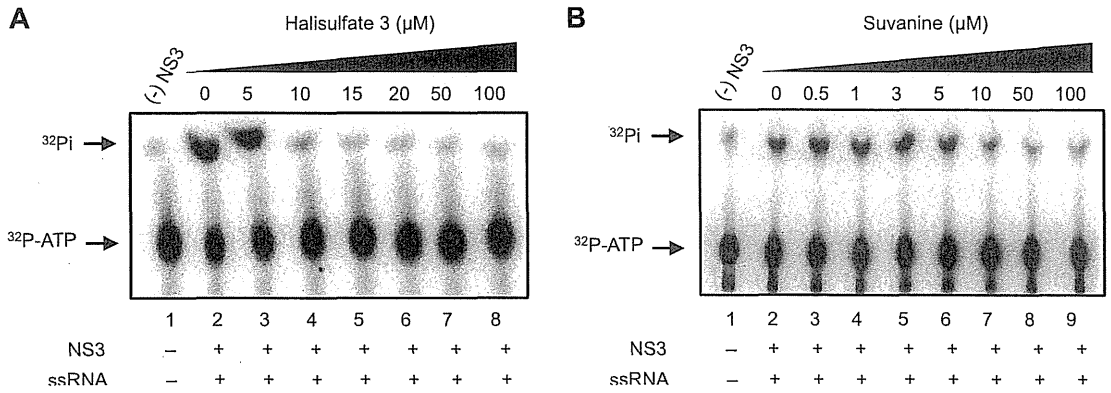

As RNA binding is required for NS3 helicase activity, the effects of hal3 and suvanine on NS3 RNA binding activity were examined by gel mobility shift assay (Figure 4). As a control, the non-specific binding of ssRNA to bovine serum albumin (BSA) was assessed (lane 2). The density of the upper bands corresponding to the NS3-ssRNA complex, which represents NS3 RNA binding activity, decreased dose-dependently in the presence of both hal3 and suvanine. RNA binding activity was calculated as the ratio of the signal intensity derived from the NS3-ssRNA complex in the sample containing the inhibitor to that in the control sample (lacking the inhibitor but containing DMSO vehicle). The IC_{50} values of hal3 and suvanine were calculated to be 8 and 3 μM, respectively. The data presented in Figures 2 and 4 reveal that the NS3 helicase and RNA binding activities decrease at similar inhibitor concentration ranges for hal3 and suvanine, suggesting that the inhibition of NS3 helicase by these compounds is associated with RNA binding activity.

Figure 4. Effects of hal3 and suvanine on NS3 RNA binding activity, assessed by autoradiography of a gel mobility shift assay using ^{32}P-labeled ssRNA. Lanes *1* and *2* contain control reactions consisting of heat-denatured ssRNA and 300 nM BSA instead of NS3, respectively. Lanes *3–9* (**A**) and *3–10* (**B**) show the RNA binding reaction with increasing concentrations (0–100 μM) of hal3 and suvanine, respectively.

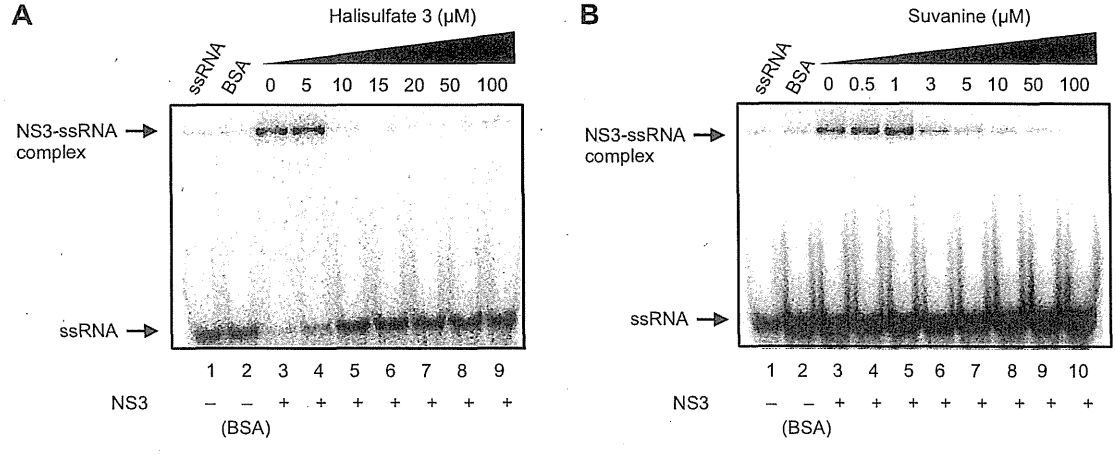

It was reported that the helicase activity of NS3 is interdependently linked to its serine protease activity [23–25]. Therefore, we examined the effects of hal3 and suvanine on NS3 serine protease activity using a fluorescence serine protease assay (Figure 5). Serine protease activity decreased in a dose-dependent manner in the presence of hal3 and suvanine, with IC_{50} values of 14 and 34 μM, respectively. Although the inhibition of the serine protease activity seems to be rather modest compared with that of the ATPase and RNA binding activities (Figures 3 and 4), the inhibition of NS3 helicase by hal3 and suvanine is likely to be also related to serine protease activity.

Figure 5. Effects of hal3 (**A**) and suvanine (**B**) on NS3 serine protease activity. The NS3 serine protease activity of samples containing inhibitor was calculated relative to control samples containing DMSO vehicle rather than inhibitor. The data are presented as means ± standard deviation of three replicates.

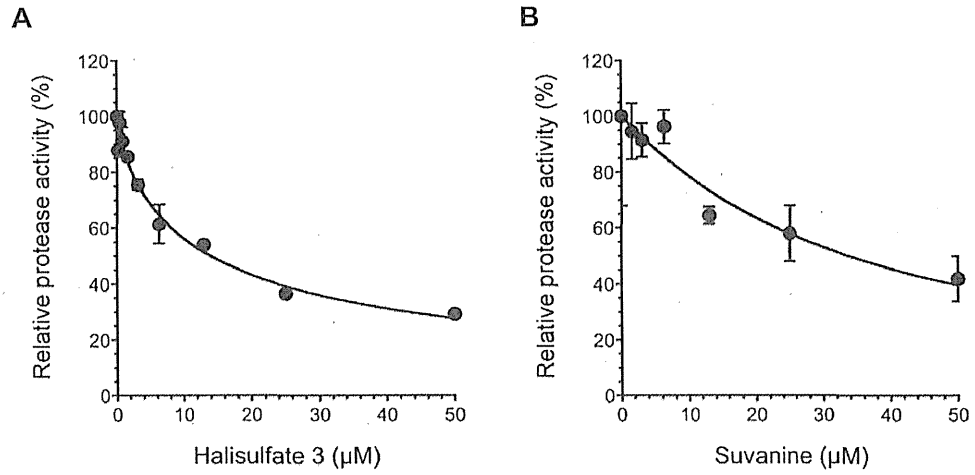

The catalytic cores of DENV and HCV NS3 helicases, which consist predominantly of ATPase and RNA binding sites, share almost identical folds and extensive structural similarity [38]. Because the substrate specificity of DENV and HCV NS3 helicases is similar [39], the dsRNA substrate and capture strand of the gel-based HCV NS3 helicase assay were also used for the gel-based DENV NS3 helicase assay (Figure 6), and helicase activity was calculated as described above. Hal3 and suvanine did not abolish DENV NS3 helicase activity, even in the presence of 100 μM of each inhibitor. This finding suggests that the inhibitory effects of hal3 and suvanine are specific to HCV NS3 helicase, and that these inhibitors bind less efficiently to any site in DENV NS3 helicase, including the catalytic core.

This study demonstrated that hal3 and suvanine inhibit the ATPase, RNA binding, and serine protease activities of NS3 (Figures 3–5). Taken together with observations that hal3 and suvanine did not inhibit DENV NS3 helicase (Figure 6), it is likely that these inhibitors do not bind to the catalytic core that contains the ATPase activity and RNA binding sites. Therefore, we conclude that hal3 and suvanine inhibit HCV NS3 helicase via interactions with allosteric sites of NS3. This likely induces conformational changes in NS3, inhibiting or abolishing its activities. Compounds with inhibitory activities against both helicase and serine protease activities have been reported previously [40]; however, there are only a small number of studies, and detailed inhibitory mechanisms are yet to be elucidated. The possible allosteric sites to which hal3 and suvanine bind could be an interface that

forms between the helicase and protease domains of NS3. Indeed, a novel small-molecule binding site at the interface between these two domains was reported recently [41]. Furthermore, the inhibitory specificity of hal3 and suvanine against HCV NS3 helicase might be explained by structural differences between HCV and DENV NS3 helicases. A specific beta-strand tethers the *C* terminus of the helicase domain to the protease domain of HCV NS3, maintaining it in a compact conformation that differs from the extended conformation of DENV NS3 helicase [42]. As only HCV NS3 helicase forms an interface between the helicase and protease domains, the specificity of hal3 and suvanine for HCV NS3 helicase would be explained by the binding of hal3 and suvanine to the interface of HCV NS3.

Figure 6. Effects of hal3 (**A**) and suvanine (**B**) on DENV NS3 helicase activity, assessed using a gel-based helicase assay. Fluorescence-labeled ssRNA and dsRNA were applied to lanes *1* and *2*, respectively. The dsRNA was incubated with NS3 in the presence of increasing concentrations of inhibitor (lanes *3*–*7*, 0–100 μM). Lanes *8* and *9* contain the control reaction mixtures in the absence of NS3, and in the presence of 15 mM ATP-gamma-S as an inhibition control, respectively.

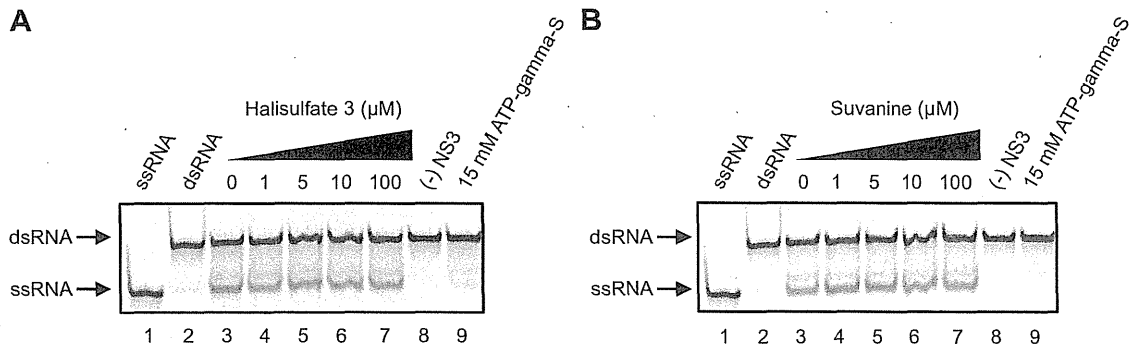

3. Experimental Section

3.1. Preparation of Extracts from Marine Organisms

Specimens of marine organisms were collected by scuba diving in Okinawa, Japan, and Sorong, Indonesia, and kept frozen until use. The specimens were chopped into small pieces, and soaked in acetone for 20 h followed by methanol for 6 h. The acetone and methanol solutions were then combined and concentrated, and residual materials were separated into ethyl acetate and aqueous layers; each layer was then dried to obtain residues.

3.2. Screening for HCV NS3 Helicase Inhibitors

The PET-based fluorescence helicase assay was performed as described previously [30]. The dsRNA substrate was prepared by annealing the 5′ BODIPY FL-labeled fluorescence strand (5′-CUAUUACCUCCACCCUCAUAACCUUUUUUUUUUUUUU-3′) to the quencher strand (5′-GGUUAUGAGGGUGGAGGUAAUAG-3′) at a 1:2 molar ratio. The dsRNA substrate contains the 3′-overhang that is necessary for the NS3 helicase to bind RNA prior to duplex unwinding. The capture strand (5′-CTATTACCTCCACCCTCATAACC-3′), which is complementary to the quencher strand, prevents the unwound duplexes from reannealing. None of the capture, quencher, or fluorescence

strands are self-complementary. The fluorescence strand was purchased from J-Bio 21 Corporation (Tokyo, Japan), and was labeled with BODIPY FL at the 5′-end via an aminohexylphosphate linker with a six-carbon spacer. The quencher and capture strands were purchased from Japan Bio Services (Saitama, Japan). The reaction mixture contained 25 mM MOPS-NaOH (pH 6.5), 3 mM $MgCl_2$, 2 mM dithiothreitol, 4 U RNasin (Promega, Madison, WI, USA), 50 nM dsRNA substrate, 100 nM capture strand, 5 mM ATP, a marine organism extract, and 240 nM NS3 in a total reaction volume of 20 μL. Each marine organism extract diluted in DMSO was added to the reaction mixture at a final concentration of 17.5–32.5 μg/mL. The full-length HCV NS3 protein with serine protease and NTPase/helicase activities was expressed and purified as described previously [43].

The reaction was started by the addition of HCV NS3 helicase, and was performed at 37 °C for 30 min using a LightCycler 1.5 (Roche Diagnostics, Basel, Switzerland). The fluorescence intensity was recorded every 5 s from 0 to 5 min, and then every 30 s from 5 to 30 min. Helicase activity was calculated as the initial reaction velocity relative to control (in the absence of a marine extract, but presence of DMSO vehicle). The IC_{50} was calculated using KaleidaGraph (Synergy Software, Reading, PA, USA) by fitting plots of % activity *vs.* [*I*] using Equation (1) unless otherwise noted [44]:

$$\% \text{ Activity} = \frac{100}{1+\left([I]/\text{IC}_{50}\right)^{h}} \quad (1)$$

where *h* is the Hill coefficient, and [*I*] is the inhibitor concentration.

3.3. Gel-Based HCV NS3 Helicase Assay

A gel-based helicase assay was performed on HCV NS3 helicases using an Alexa Fluor 488-labeled dsRNA strand and capture strand with the same nucleic acid sequences described in Section 3.2. The dsRNA substrate was prepared by annealing the 5′ Alexa Fluor 488-labeled strand (5′-CUAUUACCUCCACCCUCAUAACCUUUUUUUUUUUUUU-3′) to the complementary strand (5′-GGUUAUGAGGGUGGAGGUAAUAG-3′) at a 1:2 molar ratio. The same capture strand described in Section 3.2 was used. All nucleic acid strands were purchased from Japan Bio Services (Saitama, Japan). The reaction mixture for HCV NS3 helicase contained the same components as described in Section 3.2, with increasing concentrations of hal3 or suvanine in a reaction volume of 20 μL. The reaction was started by the addition of HCV NS3 helicase, and performed at 37 °C for 60 min using a GeneAmp PCR System 2700 (Applied Biosystems, Foster City, CA, USA). The reaction was stopped by the addition of 5 μL of helicase termination buffer containing 10 mM Tris-HCl (pH 7.5), 50 mM EDTA, 30% glycerol, 0.06% bromophenol blue, and 0.12% Orange G. The inhibition of NS3 helicase was analyzed on a 20% native Tris/borate/EDTA (TBE) polyacrylamide gel, and labeled RNAs were visualized using Typhoon 9210 (GE Healthcare, Waukesha, WI, USA). The helicase activity was calculated as the ratio of the signal intensity derived from ssRNA in the sample containing inhibitor to that in the control sample containing DMSO vehicle instead of inhibitor.

3.4. ATPase Assay

NS3 ATPase activity was determined directly by monitoring [γ-^{32}P] ATP hydrolysis by thin-layer chromatography, as described previously [45,46]. The reaction mixture contained 25 mM MOPS-NaOH

(pH 7.0), 1 mM dithiothreitol, 5 mM $MgCl_2$, 5 mM $CaCl_2$, 1 mM [γ-^{32}P] ATP (Muromachi Yakuhin, Tokyo, Japan), 300 nM NS3, 0.1 μg/μL poly (U) ssRNA (Sigma-Aldrich, St. Louis, MO, USA), and increasing concentrations of hal3 or suvanine in a volume of 10 μL. The reaction was conducted at 37 °C for 10 min, and stopped by the addition of 10 mM EDTA. Two microliters of each reaction mixture was then spotted onto a polyethyleneimine cellulose sheet (Merck, Darmstadt, Germany) and developed in 0.75 M LiCl/1 M formic acid solution for 20 min. The cellulose sheet was dried, and the released [γ-^{32}P] phosphoric acid was visualized using an Image Reader FLA-9000 and quantified using Multi Gauge software V 3.11 (Fujifilm, Tokyo, Japan). ATPase activity was calculated as the ratio of the signal intensity derived from the released Pi in the sample containing inhibitor to that in the control sample containing DMSO vehicle instead of inhibitor.

3.5. RNA Binding Assay

NS3 RNA binding activity was determined by gel mobility shift assay, as described previously [45,46]. The ssRNA (5′-UGAGGUAGUAGGUUGUAUAGU-3′) synthesized by Gene Design (Osaka, Japan) was labeled at the 5′-end with [γ-^{32}P] ATP (Muromachi Yakuhin, Tokyo, Japan) using T4 polynucleotide kinase (Toyobo, Osaka, Japan) at 37 °C for 60 min, and purified using the phenol-chloroform extraction method. The reaction mixture contained 30 mM Tris-HCl (pH 7.5), 100 mM NaCl, 2 mM $MgCl_2$, 1 mM dithiothreitol, 20 U RNasin Plus (Promega), 300 nM NS3, 0.1 nM ^{32}P-labeled ssRNA, and increasing concentrations of inhibitor in a volume of 20 μL. The reaction was performed at room temperature for 15 min. An equal volume of a dye solution containing 0.025% bromophenol blue and 10% glycerol in 0.5× TBE was then added to each reaction mixture, and samples were loaded onto a 6% native-polyacrylamide gel. The labeled RNA bands were visualized using an Image Reader FLA-9000 and quantified using Multi Gauge software V 3.11 (Fujifilm, Tokyo, Japan). RNA binding activity was calculated as the ratio of the signal intensity derived from the NS3-ssRNA complex in the sample containing hal3 or suvanine to that in the control sample containing DMSO vehicle rather than inhibitor.

3.6. Serine Protease Assay

A fluorescence NS3 serine protease assay, based on fluorescence resonance energy transfer, was conducted using reagents provided in a SensoLyte™ 520 HCV protease assay kit (AnaSpec, San Jose, CA, USA), as described previously [30]. Briefly, NS3 protein with a two-fold excess of the NS4A cofactor peptide Pep4AK was prepared in 1× assay buffer provided with the kit. HCV NS3/4A protease was mixed with increasing concentrations of inhibitor, and incubated at 37 °C for 15 min. The reaction was started by the addition of 5-FAM/QXL 520 substrate in a 20 μL total reaction volume containing 240 nM HCV NS3/4A protease and increasing concentrations of hal3 or suvanine. Reactions were then incubated at 37 °C for 120 min on a LightCycler 1.5 (Roche Diagnostics, Basel, Switzerland), and the fluorescence intensity was recorded every min for 120 min. NS3 serine protease activity was calculated as the initial reaction velocity in the sample containing inhibitor relative to the control sample containing DMSO vehicle rather than inhibitor.

3.7. Gel-Based DENV NS3 Helicase Assay

A gel-based helicase assay was performed using DENV NS3 helicases, and the Alexa Fluor 488-labeled dsRNA strand and capture strand with the same nucleic acid sequences described in the Section 3.3. DENV NS3 helicase requires a single stranded 3′ overhang to unwind dsRNA substrates in the 3′ to 5′ direction [39]; therefore, the substrate specificities of the DENV and HCV NS3 helicases are the same. The reaction mixture contained 50 mM Tris-HCl (pH 7.4), 1 mM DTT, 0.5% Tween 20, 0.25 μg/mL BSA, 2 mM $MgCl_2$, 4 U RNasin (Promega), 5 mM ATP, 50 nM dsRNA substrate, 300 nM capture strand, an inhibitor, and 240 nM DENV NS3 in a total volume of 20 μL. DENV NS3 helicase was prepared as described previously [47]. The reaction was started by the addition of DENV NS3 helicase, and was performed at 37 °C for 60 min using a GeneAmp PCR System 2700 (Applied Biosystems, Foster City, CA, USA). The reaction was then stopped by the addition of 5 μL helicase termination buffer that contained 10 mM Tris-HCl (pH 7.5), 50 mM EDTA, 30% glycerol, 0.06% bromophenol blue, and 0.12% Orange G. The inhibition of DENV NS3 helicase was analyzed on a 20% native TBE polyacrylamide gel, and the labeled RNAs were visualized using Typhoon 9210 (GE Healthcare, Waukesha, WI, USA). The helicase activity was calculated as the ratio of the signal intensity from ssRNA in the sample containing inhibitor to that in the control sample containing DMSO vehicle instead of inhibitor.

4. Conclusions

This study demonstrated that hal3 and suvanine isolated from a marine sponge inhibited NS3 helicase by suppressing the ATPase, RNA binding, and serine protease activities. Moreover, DENV NS3 helicase, which shares a catalytic core consisting mainly of ATPase and RNA binding activity sites with HCV NS3 helicase, was not inhibited by hal3 or suvanine. Therefore, it can be concluded that hal3 and suvanine inhibit HCV NS3 helicase specifically through interaction with an allosteric site of NS3 rather than the catalytic core, leading to the inhibition of all NS3 activities, presumably by inducing conformational changes. As such, it is possible that hal3 and suvanine are less likely to inhibit other cellular helicases that share a similar catalytic core to HCV NS3 helicase. This provides potentially useful information on advanced drug design strategies to identify novel NS3 helicase inhibitors that are expected to be more specific and less toxic. Experiments to address whether resistant HCV mutants emerge with the use of these compounds are underway in our laboratory.

Acknowledgments

The authors thank S. Nishikawa (AIST) for his kind gift of the expression plasmid pT7/His-NS3 containing the *N*-terminal His-tagged full-length HCV NS3. The Global COE Program "Center for Practical Chemical Wisdom" of the Ministry of Education, Culture, Sports, Science and Technology (MEXT) of Japan partially supported this study. This work was also partly supported by NUS SoM Start-up Grant (R-182-000-160-733, R-182-000-160-133) to NY.

Conflicts of Interest

The authors declare no conflict of interest.